

The Best Soules Basis for the Estimation of a Spectral Barycentre Network

François G. Meyer
 Applied Mathematics, University of Colorado at Boulder, Boulder CO 80305
fmeyer@colorado.edu
<https://francoismeyer.github.io>

February 4, 2025

Abstract

The main contribution of this work is a fast algorithm to compute the barycentre of a set of networks based on a Laplacian spectral pseudo-distance. The core engine for the reconstruction of the barycentre is an algorithm that explores the large library of Soules bases, and returns a basis that yields a sparse approximation of the sample mean adjacency matrix. We prove that when the networks are random realizations of stochastic block models, then our algorithm reconstructs the population mean adjacency matrix. In addition to the theoretical analysis of the estimator of the barycentre network, we perform Monte Carlo simulations to validate the theoretical properties of the estimator. This work is significant because it opens the door to the design of new spectral-based network synthesis that have theoretical guarantees.

keywords: Barycentre network; Soules basis; Fréchet mean; statistical network analysis

1 Introduction, problem statement, and related work

1.1 The barycentre network

The design of machine learning algorithms that can analyze "network-valued random variables" is of fundamental importance. Such machine learning algorithms often require the computation of a "sample mean" network that can summarize the topology and connectivity of a dataset of networks, $\{\mathbf{G}^{(1)}, \dots, \mathbf{G}^{(N)}\}$. Formally, we denote by \mathcal{S} the set of $\mathbf{n} \times \mathbf{n}$ symmetric adjacency matrices with nonnegative weights, and we assume that the adjacency matrix $\mathbf{A}^{(k)}$ of the network $\mathbf{G}^{(k)}$ is sampled from a probability space $(\mathcal{S}, \mathbb{P})$, with probability $\mathbb{P}(\mathbf{A}^{(k)})$. An example of a probability space, which plays an important role in this work is the stochastic block model (see Section 1.5). We equip the probability space $(\mathcal{S}, \mathbb{P})$ with a metric \mathbf{d} to quantify proximity of networks. Then, a notion of summary network is provided by the concept of *barycentre* [30], or *Fréchet mean* [5], network, $\hat{\boldsymbol{\mu}}_N[\mathbb{P}]$, which minimizes the sum of the squared distances to all the networks in the ensemble,

$$\hat{\boldsymbol{\mu}}_N[\mathbb{P}] \stackrel{\text{def}}{=} \operatorname{argmin}_{\mathbf{B} \in \mathcal{S}} \sum_{k=1}^N \mathbf{d}^2(\mathbf{B}, \mathbf{A}^{(k)}). \quad (1)$$

In this work, we propose a fast algorithm to compute the barycentre of a set of networks based on a Laplacian spectral pseudo-distance.

Before continuing, we introduce some notation. We denote by $[\mathbf{n}] \stackrel{\text{def}}{=} \{1, \dots, \mathbf{n}\}$. We use \mathbf{A} to denote the adjacency matrix of a network \mathbf{G} , and \mathbf{D} to denote the diagonal degree matrix. The symmetric normalized adjacency matrix, $\hat{\mathbf{A}} = \mathbf{D}^{-1/2} \mathbf{A} \mathbf{D}^{-1/2}$, is defined by $\hat{a}_{ij} \stackrel{\text{def}}{=} a_{ij} / \sqrt{d_i d_j}$ $d_i d_j \neq 0$, and is zero otherwise. The normalized Laplacian is defined by $\mathcal{L} \stackrel{\text{def}}{=} \text{Id} - \hat{\mathbf{A}}$. We denote by $\boldsymbol{\lambda} = [\lambda_1, \dots, \lambda_n]$ the ascending sequence of eigenvalues of \mathcal{L} .

1.2 The Laplacian spectral pseudo-distance

The metric \mathbf{d} that is chosen in (1) to compute $\widehat{\boldsymbol{\mu}}_N[\boldsymbol{\mu}]$ influences the topological characteristics that $\widehat{\boldsymbol{\mu}}_N[\boldsymbol{\mu}]$ inherits from $\{\mathbf{G}^{(1)}, \dots, \mathbf{G}^{(N)}\}$ [22]. We advocate that the distance between networks should be evaluated in the spectral domain, by comparing the eigenvalues of the normalized Laplacian, $\mathcal{L}^{(\mathbf{k})}$, of the respective networks $\mathbf{G}^{(\mathbf{k})}$. We define the Laplacian spectral pseudo-metric as the ℓ_2 norm between the vectors of eigenvalues $\boldsymbol{\lambda}(\mathcal{L})$ and $\boldsymbol{\lambda}(\mathcal{L}')$ of \mathcal{L} and \mathcal{L}' respectively,

$$\mathbf{d}(\mathcal{L}, \mathcal{L}') \stackrel{\text{def}}{=} \|\boldsymbol{\lambda}(\mathcal{L}) - \boldsymbol{\lambda}(\mathcal{L}')\|_2. \quad (2)$$

This pseudo-distance captures at multiple scales the structural and connectivity information in the networks [11, 34]. Defining a pseudo-distance in the spectral domain alleviates the difficulty of solving the node correspondence problem, and in the case of the normalized Laplacian, it makes it possible to compare networks of different sizes. When the networks are realizations of a stochastic block model, the eigenvalues of \mathcal{L} associated with each community are better separated from the bulk than the corresponding eigenvalues of $\mathbf{L} \stackrel{\text{def}}{=} \mathbf{D} - \mathbf{A}$ [9].

In spite of the advantages of the Laplacian spectral pseudo-metric, using this pseudo-metric to compute $\widehat{\boldsymbol{\mu}}_N[\mathbb{P}]$ brings about two technical obstacles. The first challenge stems from the fact that the metric is defined in the spectral domain, but the domain over which the optimization (1) takes place is the matrix domain. This leads to the definition of a realizable sequence $\boldsymbol{\lambda} = [\lambda_1, \dots, \lambda_n]$; we say that $\boldsymbol{\lambda}$ is realizable if there exists a normalized Laplacian matrix \mathcal{L} whose (ordered) eigenvalues satisfy $\boldsymbol{\lambda}(\mathcal{L}) = \boldsymbol{\lambda}$. Further, we define \mathcal{R} to be the set of realizable sequences $\boldsymbol{\lambda}$. The barycentre network $\widehat{\boldsymbol{\mu}}_N[\mathbb{P}]$ computed according to the Laplacian spectral pseudo-metric is defined by its eigenvalues, $\boldsymbol{\lambda}(\widehat{\boldsymbol{\mu}}_N[\mathbb{P}])$, which satisfy

$$\boldsymbol{\lambda}(\widehat{\boldsymbol{\mu}}_N[\mathbb{P}]) = \underset{\boldsymbol{\lambda} \in \mathcal{R}}{\operatorname{argmin}} \sum_{\mathbf{k}=1}^N \|\boldsymbol{\lambda} - \boldsymbol{\lambda}(\mathcal{L}^{(\mathbf{k})})\|_2^2. \quad (3)$$

If we relax this minimization problem, then the solution to (3) is the sample mean vector of eigenvalues, $\widehat{\boldsymbol{\mu}}_N[\boldsymbol{\lambda}] \stackrel{\text{def}}{=} \mathbf{N}^{-1} \sum_{\mathbf{k}=1}^N \boldsymbol{\lambda}(\mathcal{L}^{(\mathbf{k})})$, which is in general not realizable. Which brings us to the second difficulty in using a spectral pseudo-distance.

1.3 From the spectrum to the Laplacian

The knowledge of the eigenvalues of the barycentre network, $\boldsymbol{\lambda}(\widehat{\boldsymbol{\mu}}_N[\mathbb{P}])$, is insufficient to reconstruct a network; we need a set of eigenvectors that summarizes the distribution of eigenvectors associated with the respective Laplacian matrices $\mathcal{L}^{(\mathbf{k})}$. To address this problem, several authors have proposed to align the eigenvectors of the respective network adjacency matrices [16] or Laplacian matrices [33]. Others [15] have proposed numerical methods to find the best SBM whose eigenvalues match the sample mean eigenvalues. More generally, we are interested in the question of solving a symmetric nonnegative inverse eigenvalue problem [32].

In this work, we prove that the sample mean vector of eigenvalues, $\widehat{\boldsymbol{\mu}}_N[\boldsymbol{\lambda}]$ is in fact realizable, and we construct a Soules basis of eigenvectors that yields a sparse approximation of the sample mean adjacency matrix. We prove that when the networks are random realizations of stochastic block models (SBM), then our method always reconstructs the population mean adjacency matrix.

1.4 Content of the paper: our main contributions

The main contribution of this work is a fast algorithm to compute the barycentre of a set of networks based on a spectral pseudo-distance. The core engine is an algorithm that explores the large library of Soules bases [29, 13] (which is organized as a binary tree [12]), and returns the Soules basis that yields a sparse approximation of the sample mean adjacency matrix.

The Soules basis returned by our algorithm always leads to the reconstruction of a weighted network whose spectrum is the sample mean spectrum. We prove that in the context where the set of networks are random realizations of SBM $(\mathbf{p}, \mathbf{q}, \mathbf{n})$, then the Soules basis can be used to reconstruct the edge probability matrix \mathbf{P} associated with the SBM. This work is significant because it opens the door to the design of new spectral-based network synthesis [28, 4] that have theoretical guarantees. We publicly share our code to facilitate future work [21].

1.5 The stochastic block model

To provide theoretical guarantees to the algorithms presented in this paper, we will analyse the algorithms in the context where networks are sampled from a stochastic block model (SBM). SBMs (e.g. [1], and references therein) have both practical and theoretical relevance. On the one hand, they provide models that capture the topology of real networks that exhibit community structure, and whose theoretical properties are well understood. On the other hand, stochastic block models provide universal approximants to networks and can be used as building blocks to analyse more complex networks [2, 15, 24, 36].

We define the general stochastic block model $\text{SBM}(\mathbf{p}, \mathbf{q}, \mathbf{n})$. Let $\{\mathbf{B}_k\}, 1 \leq k \leq M$ be a partition of the vertex set $[\mathbf{n}]$ into M blocks (or communities). We define the vector $\mathbf{p} = [p_1, \dots, p_M]$ that encodes the edge probability within each community, and \mathbf{q} is the edge probability between communities. The entries $a_{ij} = a_{ji}, i < j$ of the adjacency matrix \mathbf{A} are independent (up to symmetry) and are distributed with Bernoulli distributions given by $\mathbb{P}(a_{ij} = 1) = p_m$ if i and j are in the same community $\mathbf{B}_m, 1 \leq m \leq M$, and $\mathbb{P}(a_{ij} = 1) = q$ if i and j are in distinct communities.

We often represent $\text{SBM}(\mathbf{p}, \mathbf{q}, \mathbf{n})$ by the matrix of edge probabilities, or matrix of connection probabilities, $\mathbf{P} \stackrel{\text{def}}{=} \mathbb{E}[\mathbf{A}]$. We sometimes consider a balanced version of the model where all blocks have the same size, $|\mathbf{B}_m| = \mathbf{n}/M$, (in that case we assume without loss of generality that \mathbf{n} is a multiple of M), and all the edge probabilities are equal, $p_1 = \dots = p_M$.

1.6 Organization of the paper

In the next section, we review the construction of Soules bases [29, 12] and their properties. The reader who is already familiar with Soules bases can skip to Section 3 wherein we describe the construction of the best Soules basis for the approximation of \mathbf{P} and derive the theoretical properties of the basis. In Section 4 we describe the reconstruction of the normalized Laplacian, and the adjacency matrix of the barycentre network. In section 6, we report the results of some experiments.

2 Soules Bases

Soules bases were invented to provide a solution to the following symmetric nonnegative inverse eigenvalue problem: find an orthogonal matrix Ψ such that $\Psi \text{diag}(\lambda_1, \dots, \lambda_n) \Psi^T \geq 0$, where we write $\mathbf{A} \geq 0$ if the entries of the matrix \mathbf{A} are nonnegative. The original construction [29] (see also [25]) provided a single basis. The authors in [12] realized that the transformation (4) could in fact be used to derive a library of so-called Soules-bases, each of which can be represented by a specific binary tree (see Fig. 2-Right). The Soules bases (or matrices) are orthogonal matrices that are constructed iteratively by applying a product of Givens rotations to a fixed vector ψ_1 with nonnegative entries. Alternatively, a Soules basis is constructed iteratively using a simple transformation described in the next section.

2.1 Construction of Soules Bases

The construction of a Soules basis proceeds iteratively, starting with a global normalized vector ψ_1 with nonnegative entries, whose support is the interval $I^{(1)} = [\mathbf{n}]$. This level, $\mathbf{l} = 1$, is the coarsest level. The algorithm progresses from the top level $\mathbf{l} = 1$ down to the finest level $\mathbf{l} = \mathbf{n}$. During each refinement process, a new vector $\psi_{\mathbf{l}+1}$ is created at level $\mathbf{l} + 1$, which is more localized than $\psi_1, \dots, \psi_{\mathbf{l}}$. At any given level \mathbf{l} , the set $[\mathbf{n}]$ is partitioned into \mathbf{l} intervals $I_q^{(\mathbf{l})}, 1 \leq q \leq \mathbf{l}, \cup_{q=1}^{\mathbf{l}} I_q^{(\mathbf{l})} = [\mathbf{n}]$, and $I_q^{(\mathbf{l})} \cap I_p^{(\mathbf{l})} = \emptyset$ if $p \neq q$. When progressing from level \mathbf{l} to $\mathbf{l} + 1$, one chooses one of the \mathbf{l} intervals, $I_q^{(\mathbf{l})}$, and split it into two sub intervals such that $I_q^{(\mathbf{l})} = I_q^{(\mathbf{l}+1)} \cup I_{q+1}^{(\mathbf{l}+1)}$ (see Fig. 1). The creation of $I_q^{(\mathbf{l}+1)}$ and $I_{q+1}^{(\mathbf{l}+1)}$ is associated with the construction of a new Soules vector $\psi_{\mathbf{l}+1}$. The new vector $\psi_{\mathbf{l}+1}$ oscillates over the block $I_q^{(\mathbf{l})}$: taking positive values in on $I_q^{(\mathbf{l}+1)}$, and negative values on $I_{q+1}^{(\mathbf{l}+1)}$. Specifically, if $I_q^{(\mathbf{l})} = [i_0, i_1]$, one chooses an index $k \in [i_0, i_1]$ and defines $I_q^{(\mathbf{l}+1)} \stackrel{\text{def}}{=} [i_0, k]$, and $I_{q+1}^{(\mathbf{l}+1)} \stackrel{\text{def}}{=} [k + 1, i_1]$ (see Fig. 1).

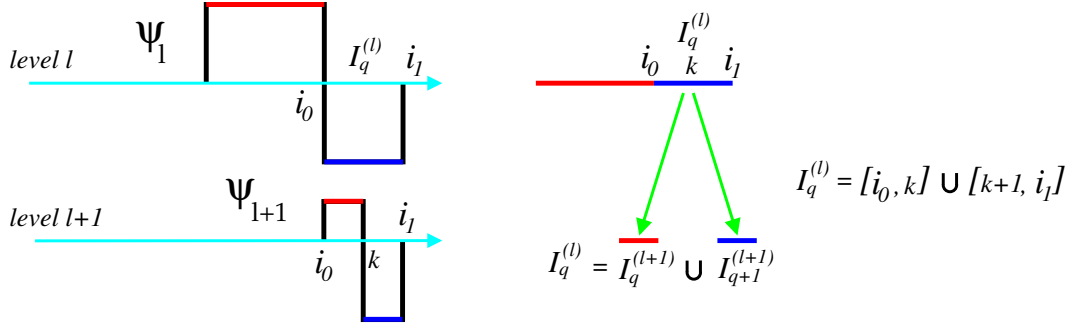


Figure 1: Left: the vector $\boldsymbol{\psi}_{l+1}$ is created by splitting a block of indices $I = [i_0, i_1]$ at level l into two sub-blocks, $[i_0, k] \cup [k+1, i_1]$ at level $l+1$. The new vector $\boldsymbol{\psi}_{l+1}$ oscillates over the block $[i_0, i_1]$. Right: interval representation of the Soules basis: a node is created in the Soules binary tree by the splitting of the interval $[i_0, i_1]$ into $[i_0, k] \cup [k+1, i_1]$

The new Soules vector $\boldsymbol{\psi}_{l+1}$ is defined by

$$\boldsymbol{\psi}_{l+1}(i) \stackrel{\text{def}}{=} \|\boldsymbol{\psi}(i_0 : i_1)\|^{-1/2} \begin{cases} \frac{\|\boldsymbol{\psi}_1(k+1 : i_1)\|}{\|\boldsymbol{\psi}_1(i_0 : k)\|} \boldsymbol{\psi}_1(i) & \text{if } i_0 \leq i \leq k \\ -\frac{\|\boldsymbol{\psi}_1(i_0 : k)\|}{\|\boldsymbol{\psi}_1(k+1 : i_1)\|} \boldsymbol{\psi}_1(i) & \text{if } k+1 \leq i \leq i_1, \end{cases} \quad (4)$$

where the vectors $\boldsymbol{\psi}_1(i_0 : i_1)$, $\boldsymbol{\psi}_1(i_0 : k)$, and $\boldsymbol{\psi}_1(k+1 : i_1)$ are n -dimensional vectors where the nonzero entries are extracted from $\boldsymbol{\psi}_1$ at the corresponding indices,

$$\begin{aligned} \boldsymbol{\psi}_1(i_0 : i_1) &= [0 \ \cdots \ 0 \ \boldsymbol{\psi}_1(i_0) \ \cdots \ \boldsymbol{\psi}_1(k) \ \boldsymbol{\psi}_1(k+1) \ \cdots \ \boldsymbol{\psi}_1(i_1) \ 0 \ \cdots \ 0], \\ \boldsymbol{\psi}_1(i_0 : k) &= [0 \ \cdots \ 0 \ \boldsymbol{\psi}_1(i_0) \ \cdots \ \boldsymbol{\psi}_1(k) \ 0 \ \cdots \ 0], \\ \boldsymbol{\psi}_1(k+1 : i_1) &= [0 \ \cdots \ 0 \ \boldsymbol{\psi}_1(k+1) \ \cdots \ \boldsymbol{\psi}_1(i_1) \ 0 \ \cdots \ 0]. \end{aligned} \quad (5)$$

The iterative subdivision process can be described using a binary tree (see Fig.2-right) where a new vector is created at each node that has two children. After n iterations, the algorithm has created $n-1$ Soules vectors, $\boldsymbol{\psi}_2, \dots, \boldsymbol{\psi}_n$, associated with the splitting of $n-1$ intervals, $I_q^{(l)}$.

We observe that two Soules vectors $\boldsymbol{\psi}_l$ and $\boldsymbol{\psi}_m$, $l \neq m$, are either nested, or they do not overlap. Indeed, either $\text{supp}(\boldsymbol{\psi}_l) \cap \text{supp}(\boldsymbol{\psi}_m) = \emptyset$, or (without loss of generality) $\text{supp}(\boldsymbol{\psi}_l) \subset \text{supp}(\boldsymbol{\psi}_m)$, $\text{supp}(\boldsymbol{\psi}_l)$ coincides with one of the two intervals in $\text{supp}(\boldsymbol{\psi}_m)$ where $\boldsymbol{\psi}_m$ is constant, and $\boldsymbol{\psi}_l$ is given by (4). In both cases, we have $\langle \boldsymbol{\psi}_l, \boldsymbol{\psi}_m \rangle = 0$. We conclude this review of the construction of the Soules bases by noting that each basis is uniquely encoded by the geometry of the corresponding binary tree (see [31] for a similar construction of Walsh-Hadamard packets). Conversely, one can tailor the tree to guide the selection of the intervals $I_q^{(l)}$ that are split, and the shape of the vectors $\boldsymbol{\psi}_l$. The algorithm described in section 3 greedily assembles a Soules basis that provides a sparse representation of the sample mean adjacency matrix. We note that there has been some recent interest in Soules bases to solve various inverse eigenvalue problems [10, 17, 23, 26].

2.2 Properties of Soules Bases

The iterative procedure leads to the construction of a set of n unit norm vectors that are mutually orthogonal. We therefore have

Lemma 1 (See [12]). *The matrix associated with n Soules vectors $[\boldsymbol{\psi}_1 \ \cdots \ \boldsymbol{\psi}_n]$ is an orthonormal matrix.*

The next result characterizes the projection operator on the span of $\{\boldsymbol{\psi}_1, \dots, \boldsymbol{\psi}_m\}$. Using (4), we can derive the following lemma with a proof by induction.

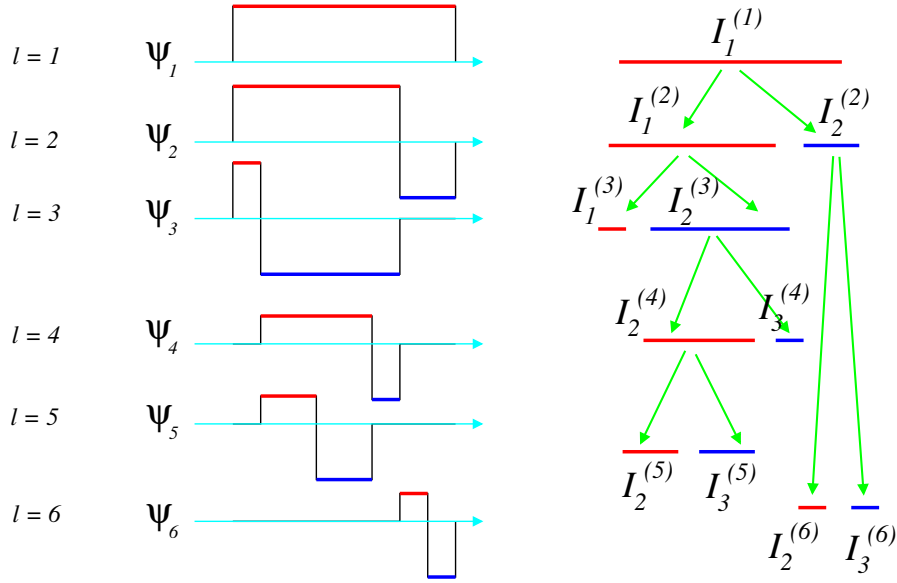


Figure 2: Left: starting from level $l = 1$, one Soules vector ψ_l is constructed at each level $l \geq 2$ by selecting and then splitting an interval $I_q^{(l)}$ over which an already existing vector ψ_m , $m \leq l$ keeps a constant value. Right: each Soules basis is associated with a binary tree. The leaves of the tree are intervals that are not split, $(I_1^{(3)}, I_2^{(5)}, I_3^{(5)}, I_3^{(4)}, I_2^{(6)}, I_3^{(6)})$. Each node with two children generates a vector ψ_l . The root of the tree ($I_1^{(1)}$) yields ψ_1 , the original vector, and ψ_2 , the vector created by the first split.

Lemma 2 (See [12]). Let $\Psi = [\psi_1 \ \cdots \ \psi_n]$ be a Soules basis constructed according to (4). Then

$$\forall m = 1, \dots, n, \quad \mathbf{E}_m \stackrel{\text{def}}{=} \sum_{q=1}^m \psi_q \psi_q^T \geq 0, \quad \text{and} \quad \sum_{q=1}^n \psi_q \psi_q^T = \text{Id}. \quad (6)$$

We now consider an ordered sequence of eigenvalues, $\lambda_1 \geq \lambda_2 \geq \cdots \geq \lambda_n$, and we define the associated diagonal matrix, $\mathbf{\Lambda} = \text{diag}(\lambda_1, \dots, \lambda_n)$. We can write $\mathbf{\Lambda}$ as the sum of $n - 1$ nonnegative diagonal matrices and a scaled version of the identity,

$$\mathbf{\Lambda} = \sum_{i=1}^{n-1} (\lambda_i - \lambda_{i+1}) \mathbf{D}_i + \lambda_n \text{Id}, \quad (7)$$

where \mathbf{D}_i is the diagonal matrix with the first i diagonal entries are equal to one, and zero afterwards, $\mathbf{D}_i = \text{diag}(1, \dots, 1, 0, \dots, 0)$. Since $\Psi \mathbf{D}_m \Psi^T = \mathbf{E}_m = \sum_{q=1}^m \psi_q \psi_q^T$, we obtain the fundamental property of Soules bases.

Lemma 3 (See [12]). Let Ψ be a Soules basis constructed according to (4). Let $\mathbf{\Lambda} = \text{diag}(\lambda_1, \dots, \lambda_n)$, where $\lambda_1 \geq \lambda_2 \geq \cdots \geq \lambda_n$. Then the off-diagonal entries of $\Psi \mathbf{\Lambda} \Psi^T$ are non-negative. In addition, if $\lambda_n \geq 0$, then $\Psi \mathbf{\Lambda} \Psi^T \geq 0$.

Remark 1. The result in lemma 3 relies on the fact that the sequence of eigenvalues is decreasing (so that $\lambda_i - \lambda_{i+1} \geq 0$ in (7)). On the other hand, the eigenvalues of \mathcal{L} are by nature ranked in ascending order. The significance of this convention is that the index k of the eigenvalue λ_k of \mathcal{L} encodes the frequency of the corresponding eigenvector. Given an ascending sequence of eigenvalues of \mathcal{L} , $0 = \lambda_1 < \lambda_2 \leq \cdots \leq \lambda_n$, we would like to apply lemma 3 to reconstruct a Laplacian matrix using a Soules basis. Since the off-diagonal entries of a normalized Laplacian \mathcal{L} are all negative, we need to work with the opposite eigenvalues. We have $0 = \lambda_1 > -\lambda_2 \geq \cdots \geq -\lambda_n$, and we can use lemma 3 to construct a matrix $\widehat{\mathcal{L}}$ given by

$$\widehat{\mathcal{L}} = \Psi \text{diag}(\lambda_1, \dots, \lambda_n) \Psi^T, \quad \text{where} \quad \widehat{\mathcal{L}}_{ij} \leq 0 \quad \text{if} \quad i \neq j. \quad (8)$$

Since we choose, $\psi_1 = n^{-1/2} \mathbf{1}$, we have $\widehat{\mathcal{L}} \mathbf{1} = \mathbf{0}$, and therefore the diagonal entries of $\widehat{\mathcal{L}}$ are nonnegative, $\widehat{\mathcal{L}}_{ii} \geq 0$. While the signs of the entries of $\widehat{\mathcal{L}}$ match those of a normalized Laplacian, there is no guarantee that $\widehat{\mathcal{L}}$ be a valid normalized Laplacian (but see a definite answer in the case of the combinatorial Laplacian, $\mathbf{L} = \mathbf{D} - \mathbf{A}$ in [10]).

This remark notwithstanding, we settle this question in section 4, in the case where all the networks are sampled from SBM $(\mathbf{p}, \mathbf{q}, \mathbf{n})$.

3 A Soules Basis for the sparse approximation of $\widehat{\mathbb{E}}_{\mathbf{N}}[\mathbf{A}]$

3.1 Approximation of the networks with a common stochastic block model

The algorithm described in the following assumes that all the networks $\{\mathbf{G}^{(1)}, \dots, \mathbf{G}^{(\mathbf{N})}\}$ in the sample can be approximated with a common stochastic block model, SBM $(\mathbf{p}, \mathbf{q}, \mathbf{n})$ with $\mathbf{p} = [\mathbf{p}_1, \dots, \mathbf{p}_M]$. The question of approximating general networks using step graphons, or SBM has received a lot of attention recently (e.g. [2, 6, 7, 15, 18, 24, 27, 36], and references therein).

In the following, we consider $\mathbf{A}^{(k)}$ to be the adjacency matrix of the SBM approximation of the network $\mathbf{G}^{(k)}$. We further assume that all the parameters of the SBM (number of blocks M , size of the blocks, $|\mathbf{B}_m|$, $1 \leq m \leq M$, edge probability density $\mathbf{p} = [\mathbf{p}_1, \dots, \mathbf{p}_M]$) can be chosen to provide a good approximation for all networks. This work focuses on the construction of the barycentre network once an SBM approximation has been computed. The study of the joint performance of the approximation with the computation of the barycentre is left for future work.

3.2 Overview of the algorithm

Given an SBM $(\mathbf{p}, \mathbf{q}, \mathbf{n})$ with $\mathbf{p} = [\mathbf{p}_1, \dots, \mathbf{p}_M]$, we describe a greedy algorithm that constructs a Soules basis, which provides a sparse approximation of the edge probability matrix \mathbf{P} . We assume that we have access to \mathbf{N} independent realizations of SBM $(\mathbf{p}, \mathbf{q}, \mathbf{n})$, represented by their adjacency matrices $\mathbf{A}^{(1)}, \dots, \mathbf{A}^{(\mathbf{N})}$. We estimate the sample mean adjacency matrix, $\widehat{\mathbb{E}}_{\mathbf{N}}[\mathbf{A}] \stackrel{\text{def}}{=} \mathbf{N}^{-1} \sum_{q=1}^{\mathbf{N}} \mathbf{A}^{(q)}$. Algorithm 1 then explores iteratively the Soules binary tree of Soules vectors from top (coarsest) level to bottom (finest) level. At each level l , the algorithm selects the interval $I_q^{(l)}$ and the split within that interval in order to minimize the residual approximation error $\|\widehat{\mathbb{E}}_{\mathbf{N}}[\mathbf{A}] - \sum_{q=1}^l \langle \boldsymbol{\psi}_q, \widehat{\mathbb{E}}_{\mathbf{N}}[\mathbf{A}] \rangle \boldsymbol{\psi}_q\|^2$ between the sample mean adjacency matrix, $\widehat{\mathbb{E}}_{\mathbf{N}}[\mathbf{A}]$, and its expansion in the Soules basis $\boldsymbol{\psi}_1, \dots, \boldsymbol{\psi}_l$.

3.3 Theoretical guarantees of the algorithm

Our analysis of algorithm 1 is performed under the assumption that the input to the algorithm is not the sample mean adjacency matrix $\widehat{\mathbb{E}}_{\mathbf{N}}[\mathbf{A}]$ but its population equivalent $\mathbb{E}[\mathbf{A}] = \mathbf{P}$. This assumption is realistic if the number of samples \mathbf{N} is large enough for some concentration phenomenon to be in effect. Our experiments (see Fig. 5) confirm the validity of this assumption. A finite sample analysis of the error bounds is left for future work.

The following lemma proves that the first M vectors of the Soules basis estimated by algorithm 1 yield the geometry of the SBM; the function \mathbf{E}_M provides an indicator function for the blocks $\mathbf{B}_k \times \mathbf{B}_k$. We will be using this lemma to prove that one can estimate the normalized Laplacian matrix associated to \mathbf{P} using the Soules basis computed with algorithm 1 and the sample mean spectrum $\widehat{\mathbb{E}}_{\mathbf{N}}[\boldsymbol{\lambda}(\mathcal{L})]$ (see lemma 5).

Lemma 4. *Let \mathbf{P} be the population mean adjacency matrix defined by*

$$\mathbf{P} = \sum_{m=1}^M (\mathbf{p}_m - \mathbf{q}) \mathbf{1}_{\mathbf{B}_m} \mathbf{1}_{\mathbf{B}_m}^T + \mathbf{q} \mathbf{J} \quad (9)$$

Let J_l , $1 \leq l \leq M$ be the leaves in the binary Soules tree (these are intervals that are no longer split, see Fig. 2-right) after M steps of algorithm 1. Then the blocks $\{\mathbf{B}_m\}$ in (9) coincide with the intervals $\{J_l\}$, and the entries of the matrix $\mathbf{E}_M \stackrel{\text{def}}{=} \sum_{m=1}^M \boldsymbol{\psi}_m \boldsymbol{\psi}_m^T$ satisfy

$$e_M(i, j) = \begin{cases} \frac{1}{|J_m|} & \text{if } (i, j) \in J_m \times J_m, \\ 0 & \text{otherwise,} \end{cases} \quad (10)$$

where $|J_m|$ is the length of the interval J_m .

Algorithm 1 Top-down exploration of the Soules binary tree.

```

1: procedure BESTSOULESBASIS( $\widehat{\mathbb{E}}_N[\mathbf{A}]$ ,  $\Psi$ )
2:    $\triangleright$  Input: sample mean adjacency matrix  $\widehat{\mathbb{E}}_N[\mathbf{A}]$ ; Output:  $\Psi$  the Soules matrix ◁
3:   for all levels  $\mathfrak{l} \in \{1, \dots, n-1\}$  do
4:      $\triangleright$  For each block  $I = [i_0, i_1]$  which was not split at level  $\mathfrak{l}$  we split it using an index  $k \in [i_0, i_1]$ , and we construct the eigenvector  $\psi_{\mathfrak{l}}$  associated with the split, and compute the coefficient  $\langle \psi_{\mathfrak{l}} \psi_{\mathfrak{l}}^T, \widehat{\mathbb{E}}_N[\mathbf{A}] \rangle$  ◁
5:     icoeff  $\leftarrow$  1  $\triangleright$  index of the tentative  $\psi_{\mathfrak{l}}$  at level  $\mathfrak{l}$ 
6:     for all blocks  $I$  at level  $\mathfrak{l}$  do  $\triangleright$  there are exactly  $\mathfrak{l}$  blocks at level  $\mathfrak{l}$ 
7:        $i_0 \leftarrow$  leftend( $I$ )  $\triangleright I = [i_0, i_1]$ 
8:        $i_1 \leftarrow$  rightend( $I$ )
9:       if ( $i_0 < i_1$ ) then  $\triangleright$  the block  $I$  is not a leaf
10:        for all  $k \in \{i_0, \dots, i_1\}$  do
11:           $\psi_{\mathfrak{l}} \leftarrow$  buildvector( $B, k$ )  $\triangleright$  use (4) to construct  $\psi_{\mathfrak{l}}$ 
12:          coeff(icoeff)  $\leftarrow$   $\langle \psi_{\mathfrak{l}} \psi_{\mathfrak{l}}^T, \widehat{\mathbb{E}}_N[\mathbf{A}] \rangle$ 
13:          icoeff  $\leftarrow$  icoeff + 1  $\triangleright$  update the index of the next tentative  $\psi_{\mathfrak{l}}$ 
14:        end for  $\triangleright$  next index  $k$  so that  $[i_0, i_1] = [i_0, k] \cup [k+1, i_1]$ 
15:      end if
16:    end for  $\triangleright$  move to the next block at level  $\mathfrak{l}$ 
17:     $\triangleright$  We have explored all the blocks at level  $\mathfrak{l}$ . We now find the block, and the split that result in the largest coefficient. We construct the eigenvector  $\psi_{\mathfrak{l}}$  associated with these choices of block and split, and we save  $\psi_{\mathfrak{l}}$  in  $\Psi$ 
18:    (bestSplit, bestBlock)  $\leftarrow$   $\underset{k \in B}{\operatorname{argmax}} \underset{B}{\operatorname{argmax}} (|\operatorname{coeff}|^2)$ 
19:     $\psi_{\mathfrak{l}} \leftarrow$  buildvector(bestBlock, bestSplit)  $\triangleright$  use (4) to construct  $\psi_{\mathfrak{l}}$ 
20:     $\Psi(:, \mathfrak{l}) \leftarrow \psi_{\mathfrak{l}}$   $\triangleright$  save  $\psi_{\mathfrak{l}}$  in the Soules basis
21:  end for  $\triangleright$  go down to a finer level
22: end procedure

```

The proof of lemma 4 is provided in section 8.1. The first ingredient of the proof is the fact that all the ψ_m are piecewise constant vectors on $[n]$; the correlation between ψ_m and \mathbf{P} is then maximal if ψ_m is perfectly aligned with a jump between two blocks (see lemma 7). The proof then proceeds with the observation that all blocks, irrespective of their size and location, can be detected by one of the ψ_m , $1 \leq m \leq M$, since the ψ_m become more and more localized as m increases.

4 The reconstruction of the normalized Laplacian

4.1 Description of the algorithm

In the following, we first present an algorithm to construct a matrix $\widehat{\mathcal{L}}$, whose spectrum is the sample mean spectrum $\widehat{\mathbb{E}}_N[\lambda(\mathcal{L})]$. We prove that in the context where the networks are sampled from a balanced SBM with $\mathbf{p}_1 = \dots = \mathbf{p}_M$ and $\widehat{\mathbb{E}}_N[\lambda(\mathcal{L})] \approx \mathbb{E}[\lambda(\mathcal{L})]$, then $\widehat{\mathcal{L}} = \mathcal{L}(\mathbf{P})$, the Laplacian of the matrix edge probability \mathbf{P} . To wit, the estimator recovers the normalized Laplacian of the expected network. Our approach combines the structural information about geometry of the block in the SBM, which is provided by lemma 4, along with the spectral information provided by the sample mean spectrum. Unfortunately, this solution, while theoretically satisfying, is numerically unstable. We propose a second estimator, which is numerically stable and has similar theoretical guarantees.

4.2 The complete reconstruction

We consider an SBM $(\mathbf{p}, \mathbf{q}, \mathbf{n})$, where $\mathbf{p} = [\mathbf{p}_1, \dots, \mathbf{p}_M]$. We assume that we have access to \mathbf{N} independent realizations of SBM $(\mathbf{p}, \mathbf{q}, \mathbf{n})$, $\mathbf{G}^{(1)}, \dots, \mathbf{G}^{(\mathbf{N})}$. For each realization $\mathbf{G}^{(q)}$, we compute the eigenvalues, $\boldsymbol{\lambda}(\mathcal{L}^{(q)})$, of the normalized Laplacian $\mathcal{L}^{(q)}$. We estimate the sample mean spectrum of the normalized Laplacian,

$$[\bar{\lambda}_1 \ \dots \ \bar{\lambda}_n]^\top \stackrel{\text{def}}{=} \widehat{\mathbb{E}}_{\mathbf{N}} [\boldsymbol{\lambda}(\mathcal{L})] = \frac{1}{\mathbf{N}} \sum_{q=1}^{\mathbf{N}} \boldsymbol{\lambda}(\mathcal{L}^{(q)}). \quad (11)$$

As explained in lemma 4, we recover the geometry of the SBM from the Soules basis $[\boldsymbol{\psi}_1 \ \dots \ \boldsymbol{\psi}_n]$ constructed by algorithm 1. We use this basis to construct the following estimator of the normalized Laplacian,

$$\widehat{\mathcal{L}} \stackrel{\text{def}}{=} \sum_{q=1}^n \bar{\lambda}_q \boldsymbol{\psi}_q \boldsymbol{\psi}_q^\top. \quad (12)$$

Because the $\boldsymbol{\psi}_q$ are Soules vectors, the spectrum of $\widehat{\mathcal{L}}$ coincides with $[\bar{\lambda}_1 \ \dots \ \bar{\lambda}_n]^\top$. We can prove more; in the context of a balanced SBM where $\mathbf{p}_1 = \dots = \mathbf{p}_M$ and in the limit of large sample size ($\widehat{\mathbb{E}}_{\mathbf{N}} [\boldsymbol{\lambda}(\mathcal{L})] \approx \mathbb{E}[\boldsymbol{\lambda}(\mathcal{L})]$), then $\widehat{\mathcal{L}}$ is equal to $\mathcal{L}(\mathbf{P})$, the normalized Laplacian associated with the edge probability matrix \mathbf{P} .

4.2.1 Theoretical guarantees of the reconstruction

Lemma 5. *Let \mathbf{P} be the edge probability matrix of a balanced SBM $(\mathbf{p}, \mathbf{q}, \mathbf{n})$ where $\mathbf{p}_1 = \dots = \mathbf{p}_M = \mathbf{p}$,*

$$\mathbf{P} = \sum_{m=1}^M (\mathbf{p} - \mathbf{q}) \mathbf{1}_{\mathbf{B}_m} \mathbf{1}_{\mathbf{B}_m}^\top + \mathbf{q} \mathbf{J}. \quad (13)$$

Then the estimator $\widehat{\mathcal{L}}$ defined in (12) is given by

$$\widehat{\mathcal{L}} = \text{Id} - \left\{ \frac{(\mathbf{p} - \mathbf{q})}{\mathbf{p} + (\mathbf{M} - 1)\mathbf{q}} \left(\sum_{m=1}^M \boldsymbol{\psi}_m \boldsymbol{\psi}_m^\top \right) + \frac{\mathbf{M}\mathbf{q}}{\mathbf{p} + (\mathbf{M} - 1)\mathbf{q}} \boldsymbol{\psi}_1 \boldsymbol{\psi}_1^\top \right\}, \quad (14)$$

and therefore $\widehat{\mathcal{L}} = \mathcal{L}(\mathbf{P})$.

The proof of lemma 5, which is provided in section 8.2, relies on estimates for the dominant eigenvalues of the symmetric normalized adjacency matrix, $\widehat{\mathbf{A}}$ [20, 3] when \mathbf{A} is the adjacency matrix of a network sampled from a balanced SBM $(\mathbf{p}, \mathbf{q}, \mathbf{n})$ with M blocks.

4.3 A partial reconstruction

In practice, the estimator of the normalized Laplacian given by $\widehat{\mathcal{L}}$ in (12) is very poor. This numerical problem is perfectly natural: the geometry and edge density of the SBM is unfortunately encoded by the smallest eigenvalues of \mathcal{L} (see lemma 4). The full expansion provided by (12) is plagued by the largest eigenvalues of \mathcal{L} , which come from the bulk created by the stochastic nature of the model, and therefore do not bring any information about the geometry of the blocks $\mathbf{B}_m \times \mathbf{B}_m$. This issue is exacerbated by the fact that the high frequency eigenvectors ($\boldsymbol{\psi}_\mathbf{l}$ with large \mathbf{l}) have small support and therefore are localized around fine scale random structures present in the sample mean adjacency matrix, $\widehat{\mathbb{E}}_{\mathbf{N}}[\mathbf{A}]$.

The expression (14) suggests that $\mathcal{L}(\mathbf{P})$ really only depends on the first M eigenvectors of the Soules basis. Therefore we propose the following estimator of the symmetric normalized adjacency matrix, $\widehat{\mathbf{A}}(\mathbf{P})$,

$$\widetilde{\mathbf{A}} \stackrel{\text{def}}{=} \frac{(\mathbf{p} - \mathbf{q})}{\mathbf{p} + (\mathbf{M} - 1)\mathbf{q}} \left(\sum_{m=1}^M \boldsymbol{\psi}_m \boldsymbol{\psi}_m^\top \right) + \frac{\mathbf{M}\mathbf{q}}{\mathbf{p} + (\mathbf{M} - 1)\mathbf{q}} \boldsymbol{\psi}_1 \boldsymbol{\psi}_1^\top. \quad (15)$$

As is shown in lemma 5, $\tilde{\mathbf{A}} = \hat{\mathbf{A}}(\mathbf{P})$ when the network is a balanced SBM $(\mathbf{p}, \mathbf{q}, \mathbf{n})$ where $\mathbf{p}_1 = \dots = \mathbf{p}_M = \mathbf{p}$. For a general SBM, one therefore proposes to estimate \mathcal{L} using a truncated reconstruction given by

$$\widehat{\mathcal{L}}_M \stackrel{\text{def}}{=} \sum_{q=1}^M \bar{\lambda}_q \boldsymbol{\psi}_q \boldsymbol{\psi}_q^\top. \quad (16)$$

In practice, one needs to estimate M , the number of eigenvalues outside the bulk. Fortunately, many estimators are available (e.g. [8, 14, 19, 35], and references therein).

4.3.1 Theoretical guarantees of the reconstruction

In the case of a balanced SBM $(\mathbf{p}, \mathbf{q}, \mathbf{n})$ where $\mathbf{p}_1 = \dots = \mathbf{p}_M = \mathbf{p}$, a simple computation reveals that

$$\widehat{\mathcal{L}}_M = \mathbf{E}_M - \frac{(\mathbf{p} - \mathbf{q})}{\mathbf{p} + (\mathbf{M} - 1)\mathbf{q}} \left(\sum_{m=1}^M \boldsymbol{\psi}_m \boldsymbol{\psi}_m^\top \right) + \frac{M\mathbf{q}}{\mathbf{p} + (\mathbf{M} - 1)\mathbf{q}} \boldsymbol{\psi}_1 \boldsymbol{\psi}_1^\top. \quad (17)$$

We recall (see lemma 4) that \mathbf{E}_M is zero outside of the blocks $\mathbf{B}_k \times \mathbf{B}_k$ of the SBM. We can therefore interpret (17) as providing the reconstruction of $\hat{\mathbf{A}}(\mathbf{P})$ given by (15) inside the blocks of the SBM, once the offset given by \mathbf{E}_M has been removed.

5 The reconstruction of the adjacency matrix

5.1 An estimator of the degree matrix

In order to recover the expected adjacency matrix, \mathbf{P} , one needs an estimate, $\hat{\mathbf{D}}$, of the degree matrix to compute $\hat{\mathbf{D}}^{1/2} \tilde{\mathbf{A}} \hat{\mathbf{D}}^{1/2}$. Lemma 4 yields an estimate of the location of the blocks in the SBM. Our estimate of the degree matrix, $\hat{\mathbf{D}}$, is computed by averaging the degrees of all the nodes in each block of the sample mean adjacency matrix, $\hat{\mathbf{E}}_N[\mathbf{A}]$

$$\hat{\mathbf{d}}_i \stackrel{\text{def}}{=} \sum_{j \in J_m} \tilde{\mathbf{a}}_{ij} \quad \text{if } i \in J_m, 1 \leq m \leq M, \quad (18)$$

where $\tilde{\mathbf{A}}$ is the estimator (15) provided by the partial reconstruction. The of \mathbf{D} estimator proves to be extremely precise.

5.2 An estimator of the adjacency matrix

We combine $\tilde{\mathbf{A}}$ given by (15) with $\hat{\mathbf{D}}$ given by (18), to derive an estimator of the edge probability matrix,

$$\hat{\mathbf{P}} \stackrel{\text{def}}{=} \hat{\mathbf{D}}^{1/2} \tilde{\mathbf{A}} \hat{\mathbf{D}}^{1/2}. \quad (19)$$

6 Experiments

We compare our theoretical analysis to finite sample estimates, which were computed using numerical simulations. The software used to conduct the experiments is publicly available [21]. All networks were generated using the SBM $(\mathbf{p}, \mathbf{q}, \mathbf{n})$ model. We first illustrate the reconstruction algorithm. For this experiment, we use $M = 4$ communities of sizes 67, 133, 71, 241 (see Fig. 3-left). The edge probability within each community was given by $\mathbf{p}_i = \mathbf{c}_i \log \mathbf{n}^2 / \mathbf{n}$, where the scaling factor \mathbf{c}_i was chosen randomly in $[1, 4]$. The edge probability across communities was given by $\mathbf{q} = 2 \log \mathbf{n} / \mathbf{n}$.

For this experiment, we use $\mathbf{N} = 1$, to wit we consider a single realisation of the SBM. This is clearly the least favorable scenario, where we expect that the estimation of the Soules basis will be the most challenging. As shown in Fig. 3-right, the first three non trivial Soules vectors accurately detected the

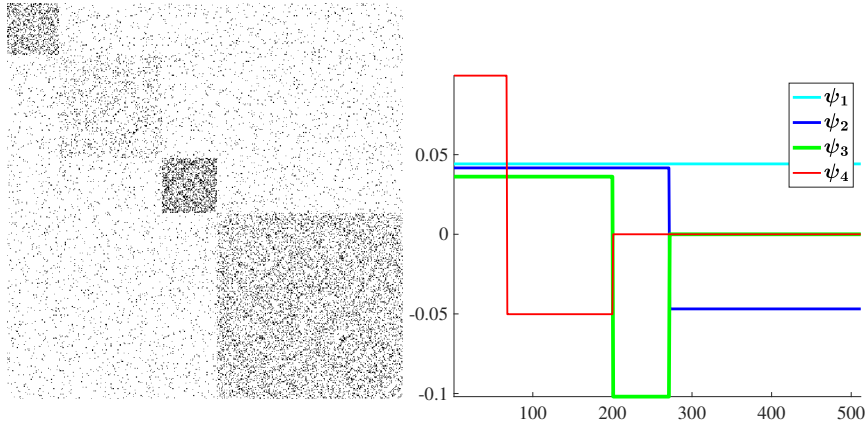


Figure 3: Left: a random realization of the SBM $(\mathbf{p}, \mathbf{q}, \mathbf{n})$ model. We have $M = 4$ communities of sizes 67, 133, 71, 241; the edge probability within community i was $\mathbf{p}_i \propto (\log \mathbf{n})^2/\mathbf{n}$, The edge probability across communities was $\mathbf{q} = 2(\log \mathbf{n})/\mathbf{n}$. Right: the first four trivial Soules vectors accurately detected the boundaries between the blocks, in spite of the very low contrast between the communities.

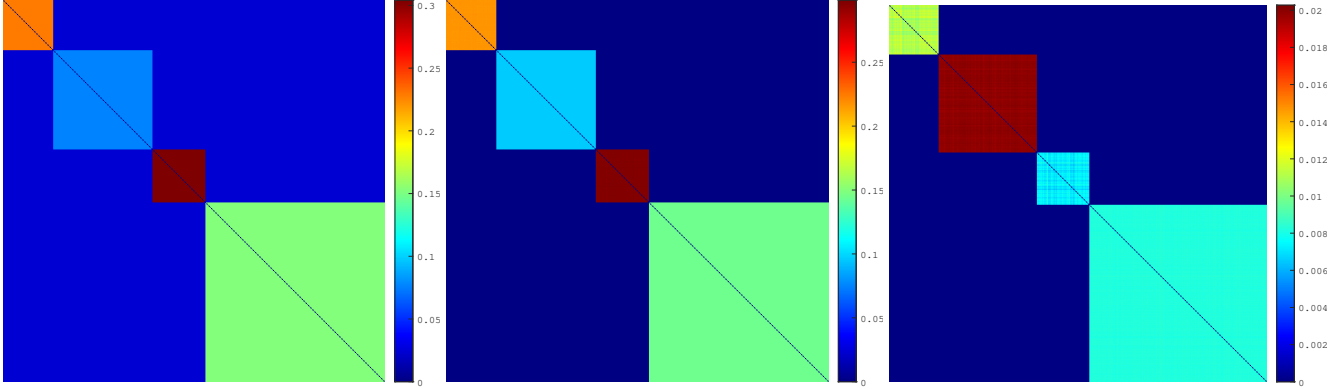


Figure 4: Left: original edge probability matrix \mathbf{P} ; center: the adjacency matrix of the barycentre network $\hat{\mathbf{P}}$, given by (19); right: the residual error between \mathbf{P} and $\hat{\mathbf{P}}$. The mean absolute error was $\mathbf{n}^{-2} \|\mathbf{P} - \hat{\mathbf{P}}\|_1 = 1.01\mathbf{e} - 05$.

boundaries between the blocks, in spite of the very low contrast between the communities (see Fig. 3-left). This numerical evidence supports the theoretical analysis of lemma 4. Figure 4 displays the original edge probability matrix \mathbf{P} (left), the reconstructed adjacency matrix, $\hat{\mathbf{P}}$, using the top 4 Soules vectors (center), and the residual error between \mathbf{P} and the reconstructed matrix $\hat{\mathbf{P}}$, and \mathbf{P} . The mean absolute error, was $\mathbf{n}^{-2} \|\mathbf{P} - \hat{\mathbf{P}}\|_1 = 1.01\mathbf{e} - 05$.

To explore the effect of the network size on the reconstruction error, we studied the effect of the network size, \mathbf{n} , on the mean absolute reconstruction error (see Fig. 5-left). We rescaled the $M = 4$ SBM model described in the previous paragraph, keeping the relative sizes of the communities the same, and increased the network size from $\mathbf{n} = 100$ to $\mathbf{n} = 1,000$. For each \mathbf{n} , we computed the mean absolute reconstruction error. As expected, the error decreases as a function of \mathbf{n} . We found $\mathbf{n}^{-2} \|\mathbf{P} - \hat{\mathbf{P}}\|_1 \propto \mathbf{n}^{-1.7}$. This experiment validates the theoretical derivations that were obtained in the limit of large network sizes, when some concentration phenomenon is in effect, and we can replace $\hat{\mathbb{E}}_N[\mathbf{A}]$ with $\mathbb{E}[\mathbf{A}] = \mathbf{P}$ in our analysis of algorithm 1.

The next experiment illustrates the effect of the number of blocks M in a balanced SBM $(\mathbf{p}, \mathbf{q}, \mathbf{n})$ when the edge probabilities are equal, $\mathbf{p}_1 = \dots = \mathbf{p}_M$. As is shown in (46), when M becomes large, then the first $M - 1$ non trivial eigenvalues λ_m of \mathcal{L} , converge to 1. Because these eigenvalues are no longer separated from the bulk, the truncated reconstruction using the Soules basis (15) becomes numerically unstable, and the reconstruction error increases (see Fig. 5-right).

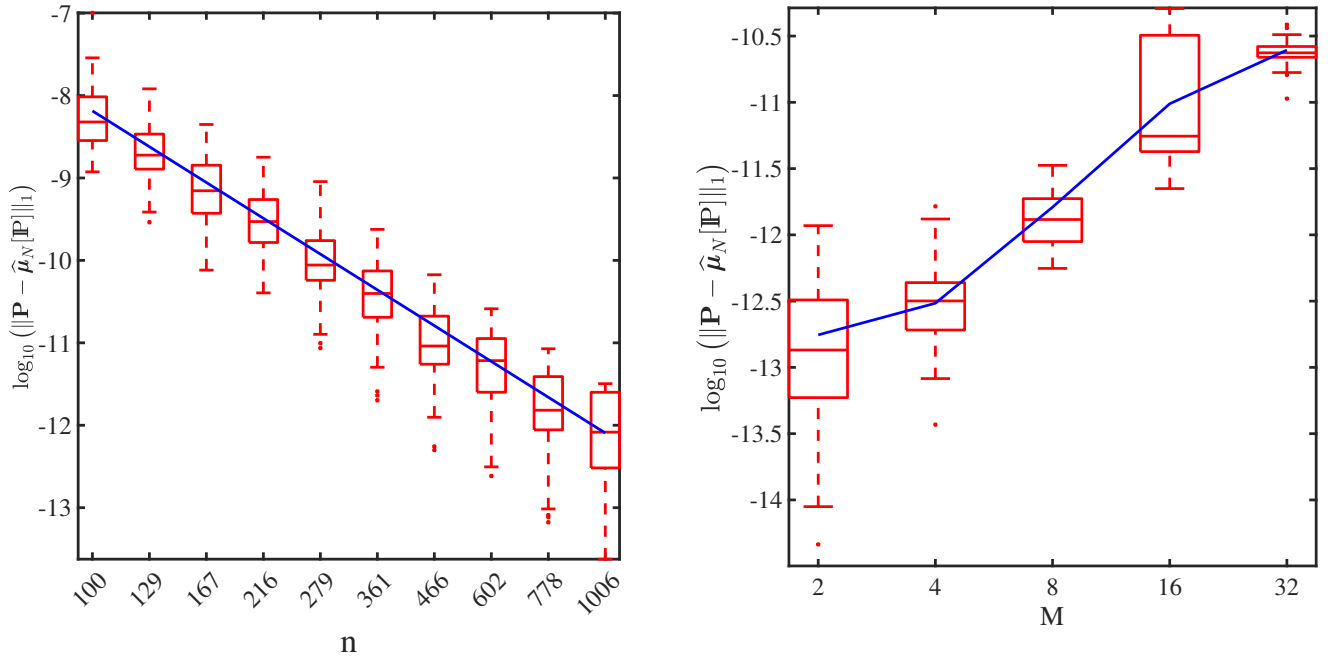


Figure 5: Left: mean absolute error $\mathbf{n}^{-2}\|\mathbf{P} - \widehat{\mathbf{P}}\|_1$ as a function of the network size, \mathbf{n} . The network is composed of $\mathbf{M} = 4$ communities, and is a scaled version of the network shown in Fig. 4. Right: mean absolute error $\mathbf{n}^{-2}\|\mathbf{P} - \widehat{\mathbf{P}}\|_1$ as a function of the number of blocks, \mathbf{M} . Each network is sampled from a balanced SBM $(\mathbf{p}, \mathbf{q}, \mathbf{n})$ with \mathbf{M} blocks and $\mathbf{p}_i = 3(\log \mathbf{n})^2/\mathbf{n}$, $\mathbf{q} = 2(\log \mathbf{n})^2/\mathbf{n}$, and $\mathbf{n} = 512$.

7 Discussion

In this work, we proposed a fast algorithm to compute the barycentre of a set of networks based on the Laplacian spectral pseudo-distance. An original contribution is an algorithm that explores the large library of Soules bases, and returns a basis that yields a sparse approximation of the sample mean adjacency matrix. Our method combines the spectral information – provided by the sample mean of the first \mathbf{M} nontrivial eigenvalues of the normalized Laplacians of the sample – with structural information given by the coarse scale Soules vectors, which are computed using the sample mean adjacency matrix.

We provided some theoretical guarantees in the context where the networks are random realizations of stochastic block models. We proved that when the networks are sampled from a balanced SBM with $\mathbf{p}_1 = \dots = \mathbf{p}_\mathbf{M}$, then $\widehat{\mathcal{L}} = \mathcal{L}(\mathbf{P})$, and our approach reconstructs the edge probability matrix. In addition to the theoretical analysis of the estimator of the barycentre network, we performed Monte Carlo simulations to validate the theoretical properties of the estimator.

Soules bases can always be used to construct non negative matrices with a prescribed set of eigenvalues. Our work is significant because we not only match the eigenvalues, but the coarse scale Soules vectors completely capture the community structure present in the network. There has not been any work that takes advantage of the binary tree structure of the Soules bases; the present paper offers for the first time a principled method to quickly explore the large library of Soules bases, and construct a Soules basis that provides a sparse approximation of the sample mean adjacency matrix. We expect that this work will open the door to the design of new spectral-based network synthesis that have theoretical guarantees.

To extend our work to larger classes of networks, one needs to compute a piecewise constant approximation to the sample mean network adjacency matrix. Our experiments (not shown) demonstrate that the algorithm of [6] provides excellent approximation for a large class of networks.

8 Additional proofs

8.1 Proof of lemma 4

The proof of lemma 4 relies on two different results. We first show that a top-down exploration of the Soules binary tree, when the first Soules vector is $\boldsymbol{\psi}_1 = \mathbf{n}^{-1/2}\mathbf{1}$, always result in a matrix $\mathbf{E}_M = \sum_{q=1}^M \boldsymbol{\psi}_q \boldsymbol{\psi}_q^\top$ that is piecewise constant on square blocks aligned along the diagonal, and zero outside of the blocks (see corollary 1). This property only relies on the fact that the sequence of $\boldsymbol{\psi}_m$ have nested supports. The second result specifically addresses the construction of each $\boldsymbol{\psi}_m$ in algorithm 1. We prove in lemma 9 that at each level \mathbf{l} , the Soules vector $\boldsymbol{\psi}_\mathbf{l}$ returned by algorithm 1 is aligned with the boundary of a block \mathbf{B}_m of the edge probability matrix \mathbf{P} . At level M , algorithm 1 has discovered all the M blocks. In the process, we prove several technical lemmata.

The tensor product $\boldsymbol{\psi}_\mathbf{l} \boldsymbol{\psi}_\mathbf{l}$

The first lemma is an elementary calculation that gives the expression of $\boldsymbol{\psi}_\mathbf{l} \boldsymbol{\psi}_\mathbf{l}^\top$

Lemma 6. We choose $\boldsymbol{\psi}_1 \stackrel{\text{def}}{=} \mathbf{n}^{-1/2}\mathbf{1}$, and denote by $\boldsymbol{\psi}_\mathbf{l}$ the Soules vector returned by algorithm 1 at level \mathbf{l} . Let $\text{supp}(\boldsymbol{\psi}_\mathbf{l}) = [i_0, i_1]$, and let k be the location of the split in $[i_0, i_1]$ such that $\boldsymbol{\psi}_\mathbf{l}|_{[i_0, k]} > 0$ and $\boldsymbol{\psi}_\mathbf{l}|_{[k+1, i_1]} < 0$ (see Fig. 1). Then,

$$\boldsymbol{\psi}_\mathbf{l} \boldsymbol{\psi}_\mathbf{l}^\top(i, j) = \frac{1}{i_1 - i_0 + 1} \begin{cases} \frac{i_1 - k}{k - i_0 + 1} & \text{if } i_0 \leq i, j \leq k \\ \frac{k - i_0 + 1}{i_1 - k} & \text{if } k + 1 \leq i, j \leq i_1 \\ -1 & \text{if } \begin{cases} i_0 \leq i \leq k, & k + 1 \leq j \leq i_1, \\ k + 1 \leq i \leq i_1, & i_0 \leq j \leq k, \end{cases} \\ 0 & \text{otherwise.} \end{cases} \quad (20)$$

Proof. The proof is an elementary calculation based on the definition of $\boldsymbol{\psi}_\mathbf{l}$ given by (4), and the observation that $\boldsymbol{\psi}_1(i) = \mathbf{n}^{-1/2}$. Indeed, we know from (4) that $\boldsymbol{\psi}_\mathbf{l}$ is piecewise constant, and given by

$$\boldsymbol{\psi}_\mathbf{l}(i) = \frac{1}{\sqrt{i_1 - i_0 + 1}} \begin{cases} \frac{\sqrt{i_1 - k}}{\sqrt{k - i_0 + 1}} & \text{if } i_0 \leq i \leq k, \\ -\frac{\sqrt{k - i_0 + 1}}{\sqrt{i_1 - k}} & \text{if } k + 1 \leq i \leq i_1, \\ 0 & \text{otherwise.} \end{cases} \quad (21)$$

The computation of the tensor product is immediate and yields the advertised result. \square

The matrix \mathbf{E}_M

In the following corollary, we describe the matrix $\mathbf{E}_M = \sum_{m=1}^M \boldsymbol{\psi}_m \boldsymbol{\psi}_m^\top$. When combined with lemma 9, we use the corollary to reconstruct the geometry of the blocks in the SBM.

Corollary 1. Let J_m be the leaves in the binary Soules tree (these are intervals that are no longer split) after M steps of algorithm 1. Then $\mathbf{E}_M \stackrel{\text{def}}{=} \sum_{m=1}^M \boldsymbol{\psi}_m \boldsymbol{\psi}_m^\top$ is equal to

$$e_M(i, j) = \begin{cases} \frac{1}{|J_\mathbf{l}|} & \text{if } (i, j) \in J_\mathbf{l} \times J_\mathbf{l}, \\ 0 & \text{otherwise.} \end{cases} \quad (22)$$

Also,

$$\begin{cases} \sum_{m=2}^M \boldsymbol{\psi}_m \boldsymbol{\psi}_m^T(\mathbf{i}, \mathbf{j}) > 0 & \text{if } \exists \mathbf{q} \in \{1, 2, \dots, M\}, (\mathbf{i}, \mathbf{j}) \in J_{\mathbf{q}} \times J_{\mathbf{q}} \\ \sum_{m=2}^M \boldsymbol{\psi}_m \boldsymbol{\psi}_m^T(\mathbf{i}, \mathbf{j}) < 0 & \text{otherwise} \end{cases} \quad (23)$$

Proof. We first observe that after M iterations of algorithm 1 there are M intervals J_m that are not split (the leaves in the binary tree shown in Fig. 2), where we count the construction of $\boldsymbol{\psi}_1$ as the first iteration of the algorithm ($M = 1$). This can be proved by induction, after observing that an iteration of algorithm 1, described by (4), turns exactly one leaf in the tree into two leaves.

Next, we prove that \mathbf{E}_M is nonnegative on each $J_l \times J_l$, $1 \leq l \leq M$. Since, each interval J_l is a leaf of the tree, the interval J_l is not further decomposed, and there exists a vector $\boldsymbol{\psi}_q$ such that $\boldsymbol{\psi}_q|_{J_l} > 0$ or $\boldsymbol{\psi}_q|_{J_l} < 0$ (see Fig. 2-right). We can therefore apply lemma 6, with $J_l = [i_0, k]$ or $J_l = [k, i_1]$, and $\boldsymbol{\psi}_q \boldsymbol{\psi}_q^T$ is constant on $J_l \times J_l$ (see (20)). All other vectors larger scale $\boldsymbol{\psi}_m$ such that $J_l \subset \text{supp}(\boldsymbol{\psi}_m)$, also keep a constant value on J_l , and therefore $\boldsymbol{\psi}_m \boldsymbol{\psi}_m^T$ is constant on $J_l \times J_l$. We conclude that \mathbf{E}_M is constant on each $J_l \times J_l$, $1 \leq l \leq M$.

We can then prove by induction that

$$\mathbf{e}_M(\mathbf{i}, \mathbf{j}) = \begin{cases} \frac{1}{|J_l|} & \text{if } (\mathbf{i}, \mathbf{j}) \in J_l \times J_l, \\ 0 & \text{otherwise.} \end{cases} \quad (24)$$

For $M = 1$ there is nothing to prove, since $\boldsymbol{\psi}_1 = n^{-1/2} \mathbf{1}$, so $\mathbf{E}_1 = n^{-1} \mathbf{J}$. Now, assume that (24) holds for $M \geq 1$, then $\mathbf{E}_{M+1} = \mathbf{E}_M + \boldsymbol{\psi}_{M+1} \boldsymbol{\psi}_{M+1}^T$, and $\boldsymbol{\psi}_{M+1}$ is created by splitting an interval J_q , so there exists $\mathbf{q} \in \{1, \dots, M\}$, such that $\text{supp}(\boldsymbol{\psi}_{M+1}) = J_q$, and $\boldsymbol{\psi}_{M+1}|_{J_m} = 0$ for all $m \neq q$. Since J_q is the only block that changes when going from M to $M + 1$, \mathbf{E}_{M+1} is equal to \mathbf{E}_M on all the other blocks. Using the induction hypothesis, we then have for all $m \neq q$,

$$\forall (\mathbf{i}, \mathbf{j}) \in J_m \times J_m, \quad \mathbf{e}_{M+1}(\mathbf{i}, \mathbf{j}) = \mathbf{e}_M(\mathbf{i}, \mathbf{j}) = \frac{1}{|J_m|}. \quad (25)$$

We are left with the computation of \mathbf{E}_{M+1} on J_q . Let us define i_0 and i_1 such that $J_q = [i_0, i_1]$, and let k be the index where J_q is split, $J_q = [i_0, k] \cup [k + 1, i_1]$. Then using lemma 6 we have for all $(\mathbf{i}, \mathbf{j}) \in J_q \times J_q$,

$$\boldsymbol{\psi}_{M+1} \boldsymbol{\psi}_{M+1}^T(\mathbf{i}, \mathbf{j}) = \frac{1}{i_1 - i_0 + 1} \begin{cases} \frac{i_1 - k}{k - i_0 + 1} & \text{if } (\mathbf{i}, \mathbf{j}) \in [i_0, k] \times [i_0, k], \\ \frac{k - i_0 + 1}{i_1 - k} & \text{if } (\mathbf{i}, \mathbf{j}) \in [k + 1, i_1] \times [k + 1, i_1], \\ -1 & \text{otherwise.} \end{cases} \quad (26)$$

From the induction hypothesis, we have for all $(\mathbf{i}, \mathbf{j}) \in J_q \times J_q$, $\mathbf{e}_M(\mathbf{i}, \mathbf{j}) = |i_1 - i_0 + 1|^{-1}$. Adding \mathbf{E}_M and $\boldsymbol{\psi}_{M+1} \boldsymbol{\psi}_{M+1}^T$ yields for all $(\mathbf{i}, \mathbf{j}) \in J_q \times J_q$,

$$\mathbf{e}_{M+1}(\mathbf{i}, \mathbf{j}) = \begin{cases} \frac{1}{k - i_0 + 1} & \text{if } (\mathbf{i}, \mathbf{j}) \in [i_0, k] \times [i_0, k], \\ \frac{1}{i_1 - k} & \text{if } (\mathbf{i}, \mathbf{j}) \in [k + 1, i_1] \times [k + 1, i_1], \\ 0 & \text{otherwise,} \end{cases} \quad (27)$$

which concludes the case for $M + 1$. By induction, (24) holds for all M .

We conclude the proof of corollary 1 by proving (23). Let $(\mathbf{i}, \mathbf{j}) \in \{1, \dots, n\} \times \{1, \dots, n\}$. If $\exists \mathbf{q} \in \{1, \dots, M\}$, such that (\mathbf{i}, \mathbf{j}) is in block $J_q \times J_q$ then $\mathbf{e}_M(\mathbf{i}, \mathbf{j}) = |J_q|^{-1}$. Also, $\boldsymbol{\psi}_q \boldsymbol{\psi}_q^T(\mathbf{i}, \mathbf{j}) = n^{-1}$, and thus

$$\sum_{m=2}^M \boldsymbol{\psi}_m \boldsymbol{\psi}_m^T(\mathbf{i}, \mathbf{j}) = \frac{1}{|J_q|} - \frac{1}{n} > 0, \quad (28)$$

since $|J_q| > 1$. Now, if (\mathbf{i}, \mathbf{j}) is not in any blocks $J_q \times J_q$, then $\mathbf{e}_M(\mathbf{i}, \mathbf{j}) = 0$, and therefore $\mathbf{e}_M(\mathbf{i}, \mathbf{j}) - \boldsymbol{\psi}_1 \boldsymbol{\psi}_1^T(\mathbf{i}, \mathbf{j}) = -n^{-1} < 0$. \square

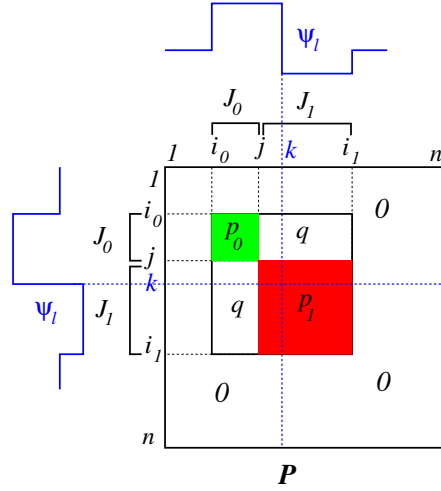


Figure 6: The vector $\boldsymbol{\psi}_l$ (in blue) is created by splitting a block of indices $I = [i_0, i_1]$ at level $l-1$ into two sub-blocks, $[i_0, k] \cup [k+1, i_1]$ at level l . We consider the matrix \mathbf{P} that is nonzero only on $[i_0, i_1] \times [i_0, i_1]$, and is piecewise constant on two blocks $J_0 \times J_0$ (in red) and $J_1 \times J_1$ (in green), where $J_0 = [i_0, j]$, and $J_1 = [j+1, i_1]$

We now prove a series of lemmata that address the performance of algorithm 1 and its ability to detect the blocks of an SBM by aligning the successive $\boldsymbol{\psi}_m$ with the block boundaries.

One iteration of algorithm 1

The next lemma studies a single iteration of algorithm 1, which leads to the construction of the Soules vector $\boldsymbol{\psi}_l$. We assume that $\text{supp}(\boldsymbol{\psi}_l) = [i_0, i_1]$, and we consider the matrix \mathbf{P} that is nonzero only on $[i_0, i_1] \times [i_0, i_1]$, and is piecewise constant on two blocks $J_0 \times J_0$ and $J_1 \times J_1$, where $J_0 = [i_0, j]$, and $J_1 = [j+1, i_1]$ (see Fig. 6),

$$\mathbf{P} = p_0(\mathbf{1}_{J_0}\mathbf{1}_{J_0}^T) + p_1(\mathbf{1}_{J_1}\mathbf{1}_{J_1}^T) + q(\mathbf{1}_{J_0}\mathbf{1}_{J_1}^T + \mathbf{1}_{J_1}\mathbf{1}_{J_0}^T). \quad (29)$$

We prove that in order to maximize $|\langle \boldsymbol{\psi}_l \boldsymbol{\psi}_l^T, \mathbf{P} \rangle|^2$, algorithm 1 must always align k (the zero-crossing of $\boldsymbol{\psi}_l$) with the jump in the SBM inside $\text{supp}(\boldsymbol{\psi}_l \boldsymbol{\psi}_l^T)$ (see Fig. 6).

Lemma 7. *Let $\boldsymbol{\psi}_l$ be the Soules vector returned by algorithm 1 at level l . Let J_0, J_1 be two contiguous non overlapping intervals such that $\text{supp}(\boldsymbol{\psi}_l) = J_0 \cup J_1$. Let \mathbf{P} be the population mean adjacency matrix defined by*

$$\mathbf{P} = p_0(\mathbf{1}_{J_0}\mathbf{1}_{J_0}^T) + p_1(\mathbf{1}_{J_1}\mathbf{1}_{J_1}^T) + q(\mathbf{1}_{J_0}\mathbf{1}_{J_1}^T + \mathbf{1}_{J_1}\mathbf{1}_{J_0}^T). \quad (30)$$

Then $|\langle \boldsymbol{\psi}_l \boldsymbol{\psi}_l^T, \mathbf{P} \rangle|^2$ is maximum if the zero-crossing of $\boldsymbol{\psi}_l$ is aligned with the location of the jump between J_0 and J_1 . Also, if $p_0 = p_1 = q$ then $\langle \boldsymbol{\psi}_l \boldsymbol{\psi}_l^T, \mathbf{P} \rangle = 0$.

Proof. The proof relies on the computation of the inner-product between a Soules tensor product $\boldsymbol{\psi}_l \boldsymbol{\psi}_l^T$ and an SBM whose support coincide with the support of $\boldsymbol{\psi}_l \boldsymbol{\psi}_l^T$. We use lemma 6, and we study two cases for the choice of $k \in [i_0, i_1]$.

We have

$$\langle \boldsymbol{\psi}_l \boldsymbol{\psi}_l^T, \mathbf{P} \rangle = p_0 \langle \boldsymbol{\psi}_l \boldsymbol{\psi}_l^T, \mathbf{1}_{J_0} \mathbf{1}_{J_0}^T \rangle + p_1 \langle \boldsymbol{\psi}_l \boldsymbol{\psi}_l^T, \mathbf{1}_{J_1} \mathbf{1}_{J_1}^T \rangle + q \langle \boldsymbol{\psi}_l \boldsymbol{\psi}_l^T, \mathbf{1}_{J_0} \mathbf{1}_{J_1}^T + \mathbf{1}_{J_1} \mathbf{1}_{J_0}^T \rangle. \quad (31)$$

Also, $\langle \boldsymbol{\psi}_l \boldsymbol{\psi}_l^T, \mathbf{1}_{J_q} \mathbf{1}_{J_r}^T \rangle = \langle \boldsymbol{\psi}_l, \mathbf{1}_{J_q} \rangle \langle \boldsymbol{\psi}_l, \mathbf{1}_{J_r} \rangle$, for $q, r \in \{0, 1\}$. We define $r_q \stackrel{\text{def}}{=} \langle \boldsymbol{\psi}_l, \mathbf{1}_{J_q} \rangle$ for $q = 0, 1$. Then

$$\langle \boldsymbol{\psi}_l \boldsymbol{\psi}_l^T, \mathbf{P} \rangle = p_0 r_0^2 + 2q r_0 r_1 + p_1 r_1^2. \quad (32)$$

The expression of the coefficients r_0 and r_1 can be derived by using (21). We give the details for the computation of r_0 , the computation of r_1 is very similar. To compute r_0 , we need to consider the two cases, $i_0 \leq k \leq j$ and $j \leq k \leq i_1$.

We recall from (21) that we always have

$$\psi_{\mathbf{l}}(i) = \frac{1}{\sqrt{i_1 - i_0 + 1}} \begin{cases} \frac{\sqrt{i_1 - k}}{\sqrt{k - i_0 + 1}} & \text{if } i_0 \leq i \leq k, \\ -\frac{\sqrt{k - i_0 + 1}}{\sqrt{i_1 - k}} & \text{if } k + 1 \leq i \leq i_1, \\ 0 & \text{otherwise.} \end{cases} \quad (33)$$

If $k \leq j$ then $\psi_{\mathbf{l}}$ changes sign over J_0 and we have

$$\begin{aligned} r_0 = \langle \psi_{\mathbf{l}}, \mathbf{1}_{J_0} \rangle &= \frac{1}{\sqrt{i_1 - i_0 + 1}} \left\{ \sum_{i=i_0}^k \frac{\sqrt{i_1 - k}}{\sqrt{k - i_0 + 1}} - \sum_{i=k+1}^j \frac{\sqrt{k - i_0 + 1}}{\sqrt{i_1 - k}} \right\} \\ &= \sqrt{\frac{(k - i_0 + 1)(i_1 - k)}{i_1 - i_0 + 1}} \left(\frac{i_1 - j}{i_1 - k} \right). \end{aligned} \quad (34)$$

If $j \leq k$ then $\psi_{\mathbf{l}}$ is positive over J_0 (this is the case for Fig. 6) and we have

$$r_0 = \langle \psi_{\mathbf{l}}, \mathbf{1}_{J_0} \rangle = \frac{1}{\sqrt{i_1 - i_0 + 1}} \sum_{i=i_0}^j \frac{\sqrt{i_1 - k}}{\sqrt{k - i_0 + 1}} = \sqrt{\frac{(k - i_0 + 1)(i_1 - k)}{i_1 - i_0 + 1}} \left(\frac{j - i_0 + 1}{k - i_0 + 1} \right). \quad (35)$$

A similar calculation yields r_1 . If $k + 1 \leq j + 1$ then $\psi_{\mathbf{l}}$ is negative over J_1 and we have

$$r_1 = -\sqrt{\frac{(k - i_0 + 1)(i_1 - k)}{i_1 - i_0 + 1}} \left(\frac{i_1 - j}{i_1 - k} \right), \quad (36)$$

and if $j + 1 \leq k + 1$ (this is the case for Fig. 6) then $\psi_{\mathbf{l}}$ changes sign over J_1 and we have

$$r_1 = -\sqrt{\frac{(k - i_0 + 1)(i_1 - k)}{i_1 - i_0 + 1}} \left(\frac{j - i_0 + 1}{k - i_0 + 1} \right). \quad (37)$$

We are now ready to evaluate $\langle \psi_{\mathbf{l}} \psi_{\mathbf{l}}^T, \mathbf{P} \rangle = p_0 r_0^2 + 2q r_0 r_1 + p_1 r_1^2$. Again, we need to consider the following two cases. If $k \leq j$ then

$$\begin{aligned} \langle \psi_{\mathbf{l}} \psi_{\mathbf{l}}^T, \mathbf{P} \rangle &= p_0 \frac{(k - i_0 + 1)(i_1 - k)}{i_1 - i_0 + 1} \left(\frac{i_1 - j}{i_1 - k} \right)^2 + p_1 \frac{(k - i_0 + 1)(i_1 - k)}{i_1 - i_0 + 1} \left(\frac{i_1 - j}{i_1 - k} \right)^2 \\ &\quad - 2q \frac{(k - i_0 + 1)(i_1 - k)}{i_1 - i_0 + 1} \left(\frac{i_1 - j}{i_1 - k} \right)^2 \\ &= \frac{(k - i_0 + 1)(i_1 - k)}{i_1 - i_0 + 1} \left(\frac{i_1 - j}{i_1 - k} \right)^2 \{p_0 + p_1 - 2q\}, \end{aligned} \quad (38)$$

which is maximum when $k = j$. In the case where if $j \leq k$ we have

$$\langle \psi_{\mathbf{l}} \psi_{\mathbf{l}}^T, \mathbf{P} \rangle = \frac{(k - i_0 + 1)(i_1 - k)}{i_1 - i_0 + 1} \left(\frac{j - i_0 + 1}{k - i_0 + 1} \right)^2 \{p_0 + p_1 - 2q\}, \quad (39)$$

which is also maximum when $k = j$. This concludes the proof that $\langle \psi_{\mathbf{l}} \psi_{\mathbf{l}}^T, \mathbf{P} \rangle$ is maximal if $k = j$. \square

The next lemma extends the previous lemma to a general edge probability matrix \mathbf{P} of an SBM, and it is used to prove lemma 9 by induction.

Lemma 8. Let \mathbf{P} be the population mean adjacency matrix defined by

$$\mathbf{P} = \sum_{m=1}^M (\mathbf{p}_m - \mathbf{q}) \mathbf{1}_{\mathbf{B}_m} \mathbf{1}_{\mathbf{B}_m}^T + \mathbf{q} \mathbf{J}, \quad (40)$$

where the M blocks \mathbf{B}_m form a partition of $[\mathbf{n}]$, $\cup_{m=1}^M \mathbf{B}_m = [\mathbf{n}]$. Then, the first split performed in algorithm 1, which is associated with $\boldsymbol{\psi}_2$ is located at the boundary between two blocks \mathbf{B}_m and \mathbf{B}_{m+1} .

Proof. Let \mathbf{k} be the index associated with the construction of $\boldsymbol{\psi}_2$ and the subdivision of $[\mathbf{n}]$. We need to prove that \mathbf{k} coincides with the endpoint of a block \mathbf{B}_m . By contradiction, if \mathbf{k} does not correspond to the boundary between two blocks, then there exists $\mathbf{i}_0 < \mathbf{i}_1$ such that $\mathbf{B}_m = [\mathbf{i}_0, \mathbf{i}_1]$ and $\mathbf{i}_0 < \mathbf{k} < \mathbf{i}_1$. Since \mathbf{P} is constant over the block $[\mathbf{i}_0, \mathbf{i}_1] \times [\mathbf{i}_0, \mathbf{i}_1]$ (see Fig. 6 with $\mathbf{p}_0 = \mathbf{p}_1 = \mathbf{q}$), lemma 7 tells us that the value of \mathbf{P} in $\mathbf{B}_m \times \mathbf{B}_m$ does not contribute to $|\langle \boldsymbol{\psi}_2 \boldsymbol{\psi}_2^T, \mathbf{P} \rangle|^2$, and algorithm 1 should not have placed \mathbf{k} in \mathbf{B}_m . \square

M iterations of algorithm 1

This last lemma guarantees that after M iterations of algorithm 1, the matrix \mathbf{E}_M associated with the first M Soules vectors recovers the block geometry.

Lemma 9. Let \mathbf{P} be the population mean adjacency matrix defined by

$$\mathbf{P} = \sum_{m=1}^M (\mathbf{p}_m - \mathbf{q}) \mathbf{1}_{\mathbf{B}_m} \mathbf{1}_{\mathbf{B}_m}^T + \mathbf{q} \mathbf{J} \quad (41)$$

Let \mathbf{J}_l , $1 \leq l \leq M$ be the leaves in the binary Soules tree (these are intervals that are no longer split) after M steps of algorithm 1. Then the M blocks $\{\mathbf{B}_m\}$ that characterize \mathbf{P} in (41) coincide with the M intervals $\{\mathbf{J}_l\}$ discovered by algorithm 1.

Proof. We prove the result by induction on M . If $M = 1$, there is nothing to prove. If $M = 2$, then lemma 8 shows that $\boldsymbol{\psi}_2$ recovers the block geometry. We assume that the result holds for all \mathbf{P} with $m \leq M$ blocks given by (41). We consider the population mean adjacency matrix \mathbf{Q} defined by

$$\mathbf{Q} = \sum_{m=1}^{M+1} (\mathbf{p}_m - \mathbf{q}) \mathbf{1}_{\mathbf{C}_m} \mathbf{1}_{\mathbf{C}_m}^T + \mathbf{q} \mathbf{J}, \quad (42)$$

where $\cup_{m=1}^{M+1} \mathbf{C}_m = [\mathbf{n}]$. Because of lemma 8, the first split of $[\mathbf{n}]$, which leads to the construction of $\boldsymbol{\psi}_2$ is aligned the boundary of a block $\mathbf{C}_{m_0} = [\mathbf{i}_0, \mathbf{k}]$. Without loss of generality, we can assume that the cut is aligned with the endpoint of \mathbf{C}_{m_0} . We can then partition $\mathbf{Q} = \mathbf{Q}_1 + \mathbf{Q}_2$, where

$$\mathbf{Q}_1 = \sum_{m=1}^k (\mathbf{p}_m - \mathbf{q}) \mathbf{1}_{\mathbf{C}_m} \mathbf{1}_{\mathbf{C}_m}^T + \mathbf{q} \mathbf{1}_{[\mathbf{k}]} \mathbf{1}_{[\mathbf{k}]}^T \quad (43)$$

and

$$\mathbf{Q}_2 = \sum_{m=k+1}^{M+1} (\mathbf{p}_m - \mathbf{q}) \mathbf{1}_{\mathbf{C}_m} \mathbf{1}_{\mathbf{C}_m}^T + \mathbf{q} \mathbf{1}_{\{\mathbf{k}+1, \dots, \mathbf{n}\}} \mathbf{1}_{\{\mathbf{k}+1, \dots, \mathbf{n}\}}^T. \quad (44)$$

Again, because of lemma 8, the next splits happen (independently) in \mathbf{Q}_1 , or \mathbf{Q}_2 . We can use the induction hypothesis to argue that all further splits will be located along the blocks in \mathbf{Q}_1 , or \mathbf{Q}_2 . After M splits, the algorithm has detected all $M + 1$ blocks. By induction, the result holds for all M . \square

Lemma 4 is then a direct consequence of lemma 9 and corollary 1.

8.2 Proof of lemma 5

Proof. Let \mathbf{P} be the edge probability matrix of a balanced SBM $(\mathbf{p}, \mathbf{q}, \mathbf{n})$ where $\mathbf{p}_1 = \dots = \mathbf{p}_M = \mathbf{p}$. The authors in [20] provide the following estimates of the eigenvalues $\lambda(\widehat{\mathbf{A}})$ of the normalized adjacency matrix, $\widehat{\mathbf{A}} = \mathbf{D}^{-1/2} \mathbf{A} \mathbf{D}^{-1/2}$,

Lemma 10 (Proposition 4.3 of [20]). *The M largest eigenvalues of $\widehat{\mathbf{A}}$ are given by*

$$\lambda_m(\widehat{\mathbf{A}}) = \left\{ \begin{array}{ll} 1 & \text{if } m = 1, \\ \frac{\mathbf{p} - \mathbf{q}}{\mathbf{p} + (\mathbf{M} - 1)\mathbf{q}} & \text{if } 2 \leq m \leq M, \\ 0 & \text{if } M + 1 \leq m \leq \mathbf{n}, \end{array} \right\} + \mathcal{O}\left(\sqrt{\frac{\log \mathbf{n}}{\mathbf{n}}}\right), \quad (45)$$

in the limit of large \mathbf{n} , almost surely [20]. Neglecting the $\mathcal{O}\left(\sqrt{\log \mathbf{n}/\mathbf{n}}\right)$ terms the eigenvalues of \mathcal{L} are given by

$$\lambda_m(\mathcal{L}) = \left\{ \begin{array}{ll} 0 & \text{if } m = 1, \\ \frac{M\mathbf{q}}{\mathbf{p} + (\mathbf{M} - 1)\mathbf{q}} & \text{if } 2 \leq m \leq M, \\ 1 & \text{if } M + 1 \leq m \leq \mathbf{n}, \end{array} \right. \quad (46)$$

in the limit of large \mathbf{n} . Substituting the expression of $\lambda_q(\mathcal{L})$ given by (46) for $\bar{\lambda}_q$ in (12), we get

$$\begin{aligned} \widehat{\mathcal{L}} &= \sum_{q=1}^{\mathbf{n}} \bar{\lambda}_q \boldsymbol{\psi}_q \boldsymbol{\psi}_q^T = \sum_{q=2}^M \bar{\lambda}_q \boldsymbol{\psi}_q \boldsymbol{\psi}_q^T + \sum_{q=M+1}^{\mathbf{n}} \bar{\lambda}_q \boldsymbol{\psi}_q \boldsymbol{\psi}_q^T \\ &= \left(1 - \frac{\mathbf{p} - \mathbf{q}}{\mathbf{p} + (\mathbf{M} - 1)\mathbf{q}}\right) \sum_{q=2}^M \boldsymbol{\psi}_q \boldsymbol{\psi}_q^T + \sum_{q=M+1}^{\mathbf{n}} \boldsymbol{\psi}_q \boldsymbol{\psi}_q^T \\ &= \sum_{q=1}^{\mathbf{n}} \boldsymbol{\psi}_q \boldsymbol{\psi}_q^T - \left\{ \frac{(\mathbf{p} - \mathbf{q})}{\mathbf{p} + (\mathbf{M} - 1)\mathbf{q}} \left(\sum_{m=1}^M \boldsymbol{\psi}_m \boldsymbol{\psi}_m^T \right) + \frac{M\mathbf{q}}{\mathbf{p} + (\mathbf{M} - 1)\mathbf{q}} \boldsymbol{\psi}_1 \boldsymbol{\psi}_1^T \right\} \\ &= \text{Id} - \left\{ \frac{(\mathbf{p} - \mathbf{q})}{\mathbf{p} + (\mathbf{M} - 1)\mathbf{q}} \left(\sum_{m=1}^M \boldsymbol{\psi}_m \boldsymbol{\psi}_m^T \right) + \frac{M\mathbf{q}}{\mathbf{p} + (\mathbf{M} - 1)\mathbf{q}} \boldsymbol{\psi}_1 \boldsymbol{\psi}_1^T \right\} \\ &= \text{Id} - \left\{ \frac{(\mathbf{p} - \mathbf{q})}{\mathbf{p} + (\mathbf{M} - 1)\mathbf{q}} \mathbf{E}_M + \frac{M\mathbf{q}}{\mathbf{p} + (\mathbf{M} - 1)\mathbf{q}} \boldsymbol{\psi}_1 \boldsymbol{\psi}_1^T \right\}, \end{aligned} \quad (47)$$

in the limit of large \mathbf{n} . In the case of a balanced SBM, we have from (22),

$$\mathbf{e}_M(i, j) = \begin{cases} \frac{M}{\mathbf{n}} & \text{if } (i, j) \in J_1 \times J_1, \\ 0 & \text{otherwise.} \end{cases} \quad (48)$$

We conclude that

$$\widehat{\mathcal{L}}_{ij} = \begin{cases} 1 - \frac{\mathbf{p}M}{\mathbf{n}(\mathbf{p} + (\mathbf{M} - 1)\mathbf{q})} & \text{if } i = j \\ -\frac{\mathbf{p}M}{\mathbf{n}(\mathbf{p} + (\mathbf{M} - 1)\mathbf{q})} & \text{if } (i, j) \in J_1 \times J_1, i \neq j, \\ \frac{\mathbf{q}M}{\mathbf{n}(\mathbf{p} + (\mathbf{M} - 1)\mathbf{q})} & \text{otherwise.} \end{cases} \quad (49)$$

We conclude the proof by computing the normalized Laplacian associated with \mathbf{P} , we have

$$\mathcal{L}(\mathbf{P}) = \text{Id} - \frac{M}{\mathbf{n}(\mathbf{p} + (\mathbf{M} - 1)\mathbf{q})} \mathbf{P} \quad (50)$$

where we neglected \mathbf{p} in the computation of the degree matrix. Whence,

$$\mathcal{L}(\mathbf{P})_{ij} = \begin{cases} 1 - \frac{\mathbf{pM}}{\mathbf{n}(\mathbf{p} + (\mathbf{M} - 1)\mathbf{q})} & \text{if } i = j \\ -\frac{\mathbf{pM}}{\mathbf{n}(\mathbf{p} + (\mathbf{M} - 1)\mathbf{q})} & \text{if } (i, j) \in \mathbf{J}_1 \times \mathbf{J}_1, i \neq j, \\ \frac{\mathbf{qM}}{\mathbf{n}(\mathbf{p} + (\mathbf{M} - 1)\mathbf{q})} & \text{otherwise.} \end{cases} \quad (51)$$

We conclude that $\widehat{\mathcal{L}}_{ij} = \mathcal{L}(\mathbf{P})_{ij}$. □

References

- [1] Emmanuel Abbe, *Community detection and stochastic block models: recent developments*, Journal of Machine Learning Research **18** (2018), no. 177, 1–86.
- [2] Edo M Airolidi, Thiago B Costa, and Stanley H Chan, *Stochastic blockmodel approximation of a graphon: Theory and consistent estimation*, Advances in Neural Information Processing Systems, 2013, pp. 692–700.
- [3] Konstantin Avrachenkov, Laura Cottatellucci, and Arun Kadavankandy, *Spectral properties of random matrices for stochastic block model*, International Symposium on Modeling and Optimization in Mobile, Ad Hoc, and Wireless Networks, 2015, pp. 537–544.
- [4] Luca Baldesi, Athina Markopoulou, and Carter T Butts, *Spectral graph forge: A framework for generating synthetic graphs with a target modularity*, IEEE/ACM Transactions on Networking **27** (2019), no. 5, 2125–2136.
- [5] Moïse Blanchard and Adam Quinn Jaffe, *Fréchet mean set estimation in the Hausdorff metric, via relaxation*, Bernoulli **31** (2025), no. 1, 432 – 456.
- [6] Stanley Chan and Edoardo Airolidi, *A consistent histogram estimator for exchangeable graph models*, International Conference on Machine Learning, PMLR, 2014, pp. 208–216.
- [7] Antoine Channarond, Jean-Jacques Daudin, and Stéphane Robin, *Classification and estimation in the Stochastic Blockmodel based on the empirical degrees*, Electronic Journal of Statistics **6** (2012), 2574 – 2601.
- [8] Yi Yu D. Franco Saldaña and Yang Feng, *How many communities are there?*, Journal of Computational and Graphical Statistics **26** (2017), no. 1, 171–181.
- [9] Shaofeng Deng, Shuyang Ling, and Thomas Strohmer, *Strong consistency, graph laplacians, and the stochastic block model*, Journal of Machine Learning Research **22** (2021), no. 117, 1–44.
- [10] Karel Devriendt, Renaud Lambiotte, and Piet Van Mieghem, *Constructing laplacian matrices with soules vectors: inverse eigenvalue problem and applications*, arXiv preprint arXiv:1909.11282 (2019), 1–26.
- [11] Claire Donnat and Susan Holmes, *Tracking network dynamics: A survey using graph distances*, The Annals of Applied Statistics **12** (2018), no. 2, 971–1012.
- [12] Ludwig Elsner, Reinhard Nabben, and Michael Neumann, *Orthogonal bases that lead to symmetric nonnegative matrices*, Linear Algebra and its Applications **271** (1998), no. 1-3, 323–343.
- [13] SD Eubanks and Judith J McDonald, *On a generalization of soules bases*, SIAM journal on matrix analysis and applications **31** (2010), no. 3, 1227–1234.
- [14] Xinjie Fan, Yuguang Yue, Purnamrita Sarkar, and Y. X. Rachel Wang, *On hyperparameter tuning in general clustering problems*, Proceedings of the 37th International Conference on Machine Learning, Proceedings of Machine Learning Research, vol. 119, 13–18 Jul 2020, pp. 2996–3007.

- [15] Daniel Ferguson and François G Meyer, *Theoretical analysis and computation of the sample Fréchet mean of sets of large graphs for various metrics*, Information and Inference **12** (2023), no. 3, 1347–1404.
- [16] Miquel Ferrer, Francesc Serratosa, and Alberto Sanfeliu, *Synthesis of median spectral graph*, Pattern Recognition and Image Analysis: Second Iberian Conference, 2005, pp. 139–146.
- [17] Aden Forrow, Francis G Woodhouse, and Jörn Dunkel, *Functional control of network dynamics using designed laplacian spectra*, Physical Review X **8** (2018), no. 4, 041043.
- [18] Thorben Funke and Till Becker, *Stochastic block models: A comparison of variants and inference methods*, PLOS ONE **14** (2019), no. 4, 1–40.
- [19] Can M. Le and Elizaveta Levina, *Estimating the number of communities by spectral methods*, Electronic Journal of Statistics **16** (2022), no. 1, 3315 – 3342.
- [20] Matthias Löwe and Sara Terveer, *Hitting times for random walks on the stochastic block model*, arXiv preprint arXiv:2401.07896 (2024), 1–26.
- [21] François G. Meyer, *The Best Soules Basis for the Estimation of a Spectral Barycentre Network*, <https://github.com/francoismeyer/soules-spectral-barycentre-graph>, 2025.
- [22] François G. Meyer, *When does the mean network capture the topology of a sample of networks?*, Frontiers in Physics **12** (2024), 1–11.
- [23] Sara Nicoletti, Timoteo Carletti, Duccio Fanelli, Giorgio Battistelli, and Luigi Chisci, *Generating directed networks with prescribed laplacian spectra*, Journal of Physics: Complexity **2** (2020), no. 1, 015004.
- [24] Sofia C Olhede and Patrick J Wolfe, *Network histograms and universality of blockmodel approximation*, Proceedings of the National Academy of Sciences **111** (2014), no. 41, 14722–14727.
- [25] Hazel Perfect and Leon Mirsky, *Spectral properties of doubly-stochastic matrices*, Monatshefte für Mathematik **69** (1965), 35–57.
- [26] Ievgen Redko, Marc Sebban, and Amaury Habrard, *Non-negative matrix factorization meets time-inhomogeneous markov chains*, OPT2020: 12th Annual Workshop on Optimization for Machine Learning, 2020.
- [27] Hannu Reittu, Ilkka Norros, Tomi Rätty, Marianna Bolla, and Fülöp Bazsó, *Regular decomposition of large graphs: Foundation of a sampling approach to stochastic block model fitting*, Data Science and Engineering **4** (2019), 44–60.
- [28] Alana Shine and David Kempe, *Generative graph models based on Laplacian spectra?*, The World Wide Web Conference, ACM, 2019, pp. 1691–1701.
- [29] George W Soules, *Constructing symmetric nonnegative matrices*, Linear and Multilinear Algebra **13** (1983), no. 3, 241–251.
- [30] Karl-Theodor Sturm, *Probability measures on metric spaces of nonpositive*, Heat kernels and analysis on manifolds, graphs, and metric spaces **338** (2003), 357.
- [31] Christoph M Thiele and Lars F Villemoes, *A fast algorithm for adapted time–frequency tilings*, Applied and Computational Harmonic Analysis **3** (1996), no. 2, 91–99.
- [32] Edwin R Van Dam and Willem H Haemers, *Developments on spectral characterizations of graphs*, Discrete Mathematics **309** (2009), no. 3, 576–586.
- [33] David White and Richard C Wilson, *Spectral generative models for graphs*, 14th International Conference on Image Analysis and Processing (ICIAP 2007), IEEE, 2007, pp. 35–42.

- [34] Peter Wills and François G Meyer, *Metrics for graph comparison: a practitioner's guide*, PLoS ONE **15(2)** (2020), 1–54.
- [35] Bowei Yan, Purnamrita Sarkar, and Xiuyuan Cheng, *Provable estimation of the number of blocks in block models*, International Conference on Artificial Intelligence and Statistics, PMLR, 2018, pp. 1185–1194.
- [36] Jean-Gabriel Young, Guillaume St-Onge, Patrick Desrosiers, and Louis J Dubé, *Universality of the stochastic block model*, Physical Review E **98** (2018), no. 3, 032309.